

# How to drive roAp stars

Alfred Gautschy,<sup>1</sup> Hideyuki Saio<sup>2</sup> and Housi Harzenmoser<sup>1</sup>

<sup>1</sup>*Astronomisches Institut der Universität Basel, Venusstr.7, CH-4102 Binningen, Switzerland*

<sup>2</sup>*Astronomical Institute, Tohoku University, Sendai, Japan*

Accepted 1998 July 3. Received 1998 May 27; in original form 1998 April 15

## ABSTRACT

Rapidly oscillating Ap stars constitute a unique class of pulsators with which to study non-radial oscillations under some – even for stars – unusual physical conditions. These stars are chemically peculiar, they have strong magnetic fields and they often pulsate in several high-order acoustic modes simultaneously. We discuss here an excitation mechanism for short-period oscillation modes based on the classical  $\kappa$  mechanism. We particularly stress the conditions that must be fulfilled for successful driving. Specifically, we discuss the roles of the chemical peculiarity and strong magnetic field on the oscillation modes and what separates these pulsators from  $\delta$  Scuti and Am-type stars.

**Key words:** stars: chemically peculiar – stars: general – stars: magnetic fields – stars: oscillations.

## 1 CHARACTERIZING THE BREED

Rapidly oscillating Ap (roAp) stars constitute a low-temperature subgroup of the chemically peculiar A-type (Ap) stars with strong Sr, Cr and Eu overabundances. The first star of this class, HD 101065, was discovered photometrically in 1978 by Kurtz (Kurtz 1978; Kurtz & Wegner 1979). Presently, the group counts about 30 members. The periods of the light variability, which can be multi-periodic, range from roughly 4 to 16 minutes. As the roAp stars lie in the instability strip close to the main sequence they are thought to have masses between 1.5 and 2  $M_{\odot}$ . Therefore, the short periods must be interpreted as high radial-order  $p$  modes. The amplitudes of variability in the blue, where they are largest, stay below about a hundredth of a magnitude.

The roAp stars show strong surface magnetic fields exceeding frequently some kilogauss (cf. Mathys & Hubig 1997) with the magnetic axis being inclined relative to the rotation axis of the star. The rotation with periods above 2 days leads, therefore, to a modulation of the magnetic field strength. This property gave rise to the *oblique rotator* model (Stibbs 1950). From the temporal phase behaviour of the magnetic field during a rotation period, a dominant dipole topology was derived for the global magnetic fields of these stars.

The observed chemical peculiarities are interpreted as being a very superficial phenomenon which is restricted to the upper stellar atmosphere. It is commonly believed that the strong magnetic field suppresses turbulent motion which otherwise quickly destroys any diffusively built up segregation of atomic species that react differently on the prevailing stellar radiation field (e.g. Michaud 1980; Vauclair & Vauclair 1982; Alecian 1986). None of the available diffusion theories reproduces, however, quantitatively the observed variety of peculiar-star characteristics with a satisfactory low number of freely tunable parameters.

The short-period oscillation amplitudes of the roAp stars are temporally not stable but they vary cyclically in phase with the magnetic field modulation. The variability is in accordance with the postulation of dipole oscillation-modes being aligned with the magnetic axis of the roAp stars which changes its aspect angle during the rotation period of the star. This picture – called the *oblique pulsator* model – is furthermore supported by phase jumps of the pulsational phase at quadrature of the magnetic axis with respect to the line of sight. If the temporal variation of the pulsation is parametrized by  $\cos(\omega t + \varphi)$ , then the phase  $\varphi$  jumps by  $\pi$  radians at the moment of magnetic polarity reversal; and this is just what is observed (cf. Kurtz 1990).

The roAp variability is unique in several respects. Despite these stars sharing their territory in the instability strip with  $\delta$  Sct stars, they oscillate with much shorter periods. Much higher overtones are obviously excited in roAp stars. The mode density in the corresponding frequency domain is high, and it remains unclear what selection mechanism is picking out the very low number of observed oscillation modes. The spherical degrees of the modes identified in some cases (e.g. Kurtz 1990) were axisymmetric dipole modes. In general, they must definitely all be axisymmetric, low- $\ell$  modes.

Rotation and magnetic field of the roAp stars cause the  $m$ -degeneracy of the oscillation frequencies to be lifted. From the magnitude of the frequency splitting and the amplitudes of the multiplet components, aspect angles of the rotation and magnetic axis and spatially integrated magnetic field strengths can be deduced. If several radial orders of oscillation modes are observable (as e.g. in HR 1217, Kurtz, Schneider & Weiss 1985) frequency spacings can be deduced. As roAp stars oscillate in high radial orders and low spherical degree, asymptotic pulsation theory, together with other (spectroscopic, photometric, astrometric) observables might constrain global stellar parameters such as mass and age (cf. Christensen-Dalsgaard 1988; Brown et al. 1994).

The lifetimes of oscillation modes in roAp stars range from days to years. For long-lived modes, cyclically (but not periodic) varying oscillation frequencies on the time-scale of months were reported recently (Kurtz et al. 1994, 1997). The origin of these shifts is unclear. Speculations, however, tend towards the action of magnetic activity-cycles as seen on the sun. All in all, the roAp stars constitute a unique laboratory to test important domains of stellar pulsation theory and of stellar-hyromagnetics communicated through oscillations. For more details we refer to recent reviews which addressed comprehensively most – theoretical as well as observational – aspects of roAp stars: Kurtz (1990), Shibahashi (1991), Matthews (1997).

In Section 2 we address the stellar evolution aspect of the roAp stars and introduce the models with which we worked in our analyses. Section 3 deals with the non-adiabatic oscillation spectra of the roAp stars and the possible underlying excitation mechanism. Success and limitations of our work are critically evaluated and compared with results in the literature in Section 4. Finally, we devote an Appendix to the comparison of adiabatic and non-adiabatic oscillation spectra.

## 2 ASPECTS OF STRUCTURE AND EVOLUTION

The overlapping of the  $\delta$  Sct variables and of roAp stars in the instability strip on the HR diagram suggests that the latter have similar masses and that they are also in a comparable evolutionary stage. This is additionally supported by the asymptotic frequency separations (cf. Appendix) which, for  $\delta$  Sct-like stars, are compatible with those seen in roAp stars (e.g. Gabriel et al. 1985; Shibahashi & Saio 1985; Heller & Kawaler 1988). Therefore, we analyzed stellar models – representing roAp stars – with masses between 1.5 and 1.87  $M_{\odot}$  during the main-sequence and the early hydrogen shell-burning evolutionary phase (cf. Fig. 1).

Referring to *Hipparcos* observations, North et al. (1997) attempted recently to pin down the location of the roAp stars on the HR diagram. The result is plotted in Fig. 1 with grey shading. The dark grey area enclosed the mean values obtained for the sample of 14 stars. The lighter grey encloses the maximum extensions of the error bars specified in North et al. (1997). Their data suggest that stars with masses above roughly 1.6  $M_{\odot}$  could become roAp stars under suitable conditions mainly during their main-sequence stage. The dotted line in Fig. 1 indicates the position of the observed blue edge for  $\delta$  Sct variables. It is evident that an overlap exists; therefore, roAp and  $\delta$  Sct stars appear to share common ground.

For reference, the locus of  $\nu_0 = \text{const.}$  is plotted on the HR diagram in Fig. 1. The mathematical definition of  $\nu_0$  – the asymptotic frequency spacing of equal-degree modes – is given in the Appendix. The determination of this observable, together with a reliable temperature measure, constitutes an important characterization of a star. The  $\nu_0$  values of our models are listed in Table 1.

The stellar evolution computations for this study were performed with the Basel stellar evolution code using the microphysics described in Gautschy, Ludwig & Freytag (1996). The homogeneous chemical composition of the stellar models on the ZAMS was in all cases  $X = 0.7$ ,  $Y = 0.28$ . When evolving the stars we did not account for any chemical peculiarity. We assumed that an atmosphere with a prescribed  $T-\tau$  relation is overlying the stellar photosphere where the stellar structure computations stopped. Any changes in chemical composition and molecular weight

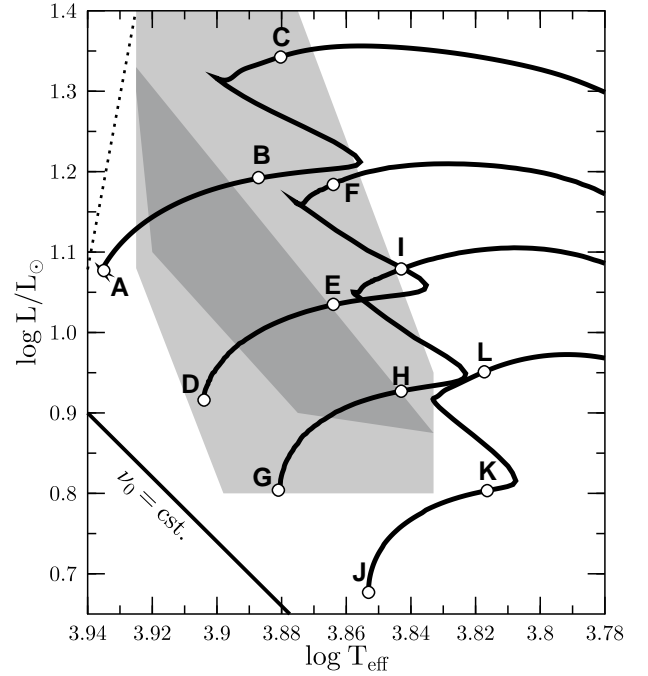


**Figure 1.** Hertzsprung-Russell diagram with the loci of the early tracks of main-sequence and early post-main sequence evolution of stars with 1.5, 1.6, 1.7, and 1.87  $M_{\odot}$ . The positions along the tracks where stellar models were analyzed for their oscillation behavior are marked with capital letters. The corresponding parameters are listed in Table 1. The grey areas denote the map of observed roAp stars onto the HR plane as published by North et al. (1997). For details see the text. The dotted line indicates the location of the observed blue edge of  $\delta$  Sct stars.

which characterize Ap-star peculiarity were restricted to these atmosphere calculations. Descriptions and results of specific choices are presented in Section 3. Furthermore, we did not consider effects of a dipole magnetic field in the computation of the stellar structure. In this respect it is worthwhile to notice that even a kilogauss non-potential field is hardly of relevance for most of the star: Fig. 2 shows the logarithm of the ratio of the magnetic pressure to the total pressure at the magnetic pole (for a dipole field) for stellar model B. Evidently, the magnetic pressure exceeds the hydrostatic pressure in the very outermost regions only. Since the the stellar envelopes of the stellar models corresponding to roAp stars are mainly radiative they approach quickly the radiative-zero solution. Therefore, surface information is not communicated to the deep interior which drives the evolution of the star. The run of  $\beta$  in

**Table 1.** Stellar parameters of models used for stability analyses.

Model	log	log $L/L_{\odot}$	$M/M_{\odot}$	$\nu_0/\mu\text{Hz}$	$10^7 \times 3GM/R^3$
A	3.936	1.086	1.87	88.36	5.626
B	3.884	1.240	1.87	51.46	1.611
C	3.880	1.352	1.87	39.37	1.036
D	3.904	0.916	1.70	89.89	5.917
E	3.864	1.035	1.70	56.56	2.257
F	3.864	1.170	1.70	44.26	1.349
G	3.880	0.804	1.60	90.30	5.967
H	3.843	0.927	1.60	57.46	2.308
I	3.843	1.079	1.60	44.77	1.365
J	3.853	0.686	1.50	90.79	5.712
K	3.816	0.812	1.50	57.67	2.217
L	3.816	0.960	1.50	45.34	1.348

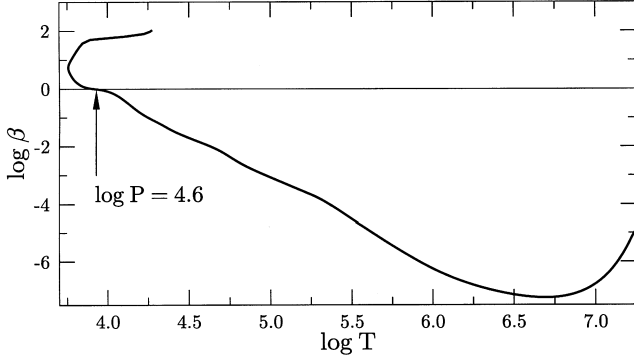


**Figure 2.** Logarithm of  $\beta$ , the ratio of magnetic pressure to total pressure throughout a star in the direction of the dipole magnetic pole. The surface magnetic field strength is chosen to be  $10^3$  G. The stellar model corresponds to model B which is characterized in Table 1.

Fig. 2 stops at the outer edge of the convective central region where the dipole nature probably breaks down.

From the stellar evolutionary sequences we selected a few models on which the stellar oscillation computations were performed. For each of the tracks – 1.5, 1.6, 1.7, and  $1.87 M_{\odot}$  – we selected two models each in the core hydrogen-burning phase and one in the early hydrogen shell-burning stage as representatives of roAp stars. Table 1 lists, for models A to L, some relevant stellar and oscillatory parameters.

### 3 THE RAPID OSCILLATIONS OF Ap STARS

In this section we focus on pulsational aspects of roAp stars. First, we address their oscillation-frequency spectra and the problems they pose in understanding the underlying stellar models. The later part of Section 3 is devoted to non-adiabatic aspects. In particular we suggest an excitation mechanism for the observed high-order  $p$  modes.

The frequently occurring dimensionless frequencies  $\sigma = (\sigma_R, \sigma_I)$  are normalized by  $\sqrt{3GM_*/R_*^3}$ . All the numerical computations of oscillation properties were performed with codes similar to the one described in Gautschy et al. (1996).

#### 3.1 Oscillation-mode physics

To get an impression of the mode cavities in stars it is appropriate to plot the characteristic frequencies  $\sigma_C$ . They separate the spatially propagative from the evanescent regions in a star (see e.g. Unno et al. 1989). We compute the dispersion relation of the adiabatic Cowling equations assuming a plane wave with a spatial behaviour of  $\exp(ikx)$  in any perturbed physical quantity, where we use  $x \equiv r/R_*$ . Searching for the loci of  $\text{Real}(k) = 0$  leads to a quadratic for  $\sigma_C^2$ :

$$\sigma_{C\pm}^2 = \frac{-B \pm \sqrt{D}}{\mathcal{N}}, \quad (1)$$

where we define

$$\mathcal{A} \equiv \left[ V \left( \frac{2}{\Gamma_1} - 1 \right) - 3 \right]^2, \quad \mathcal{B} \equiv -\frac{A^*V}{\Gamma_1} - \ell(\ell+1) - \frac{\mathcal{A}}{4},$$

$$\mathcal{D} \equiv \mathcal{B}^2 - \frac{4\ell(\ell+1)A^*V}{\Gamma_1}, \quad \mathcal{N} \equiv \frac{6c_1V}{\Gamma_1}.$$

The quantity  $A^* = -V(1/\Gamma_1 - d \log \rho / d \log P)$  is essentially the

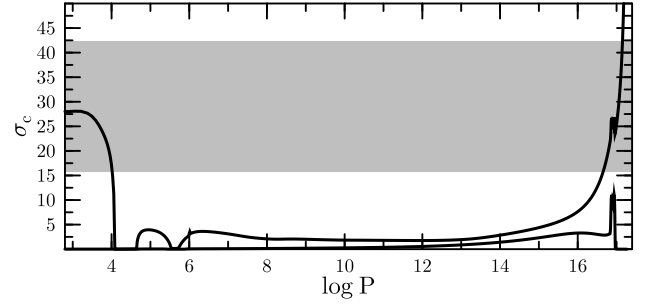


**Figure 3.** Characteristic frequencies of dipole modes for model B as function of depth which is measured in  $\log P$ . The grey-filled area covers the observed oscillation-frequency domain of roAp stars.

Schwarzschild determinant. For the meaning of the remaining symbols we refer to Unno et al. (1989).

As an example of the propagation properties of dipole modes in roAp-like stars we show in Fig. 3 the characteristic frequencies of stellar model B which is our slightly evolved  $1.87 M_{\odot}$  star. The upper and lower lines represent  $\sigma_{C+}$  and  $\sigma_{C-}$ , respectively. An oscillation mode with frequency  $\sigma$  propagates spatially as a  $p$  mode in the regions where  $\sigma$  exceeds the larger value of  $\sigma_C$ . The dominant features of the upper  $\sigma_C$  line are the two depressions in the superficial regions which are caused by partial ionization of H and He ( $4 < \log P < 4.7$ ) and  $\text{He}^+$  ( $5.5 < \log P < 5.8$ ). The top of the H/He ionization zone reaches into the photosphere. Furthermore, the steep composition gradient which builds up at the outer edge of the nuclear burning core causes the glitch in  $\sigma_C$  at about  $\log P = 16.8$ . The influence on the cavities of the composition change is even more pronounced in the lower  $\sigma_C$  curve which traces the upper boundary for the propagation region of the  $g$  modes.

The oscillation frequency domain observed in roAp stars is marked by the grey area shown in Fig. 3. We see that all the modes in the appropriate frequency range are pure acoustic modes. A slight influence on the mode spectrum from the steep molecular-weight ( $\mu$ ) gradient at the outer edge of the nuclear burning convective core can be expected.

After the roAp variability was interpreted to be a result of high-order acoustic oscillation modes, the magnitude of the critical frequency ( $\sigma_C$ ) in the stellar atmosphere, i.e. at the outer boundary of the oscillation cavity, became a point of concern. The superficial acoustic cut-off frequency,  $\sigma_{ac}$ , which corresponds to  $\sigma_C$  there, determines if a wave with frequency  $\sigma$  is reflected (if  $\sigma_R < \sigma_{ac}$ ) or if it is partially transmitted (if  $\sigma_{ac} < \sigma_R$ ) and therefore loses part of its energy into the atmosphere. Stellar models which are appropriate for roAp stars show the convection zone induced by H/He ionization to reach up to the stellar photosphere. At the photosphere the acoustic wave propagation is determined by the run of the Brunt-Väisälä frequency; which is imaginary in the convectively unstable layers. To find the outer edge of the acoustic cavity, *some* atmospheric modelling is necessary. In other words, the action of the outer boundary condition is dominated by the peculiarities in the optically thin radiative layers. The use of standard (e.g. Eddington-grey)  $T-\tau$  relations leads to rather low cut-off frequencies. Many of the observed oscillation frequencies lie above the cut-off so that some mode energy is lost from the star (cf. Fig. 3). If the cut-off frequency in roAp stars were indeed that low, then the excitation mechanism would have to be very efficient to over-compensate the modal leak into the atmosphere.

To resolve the dilemma of the low cut-off frequencies at the surfaces, considerable efforts went into hypothesizing physical

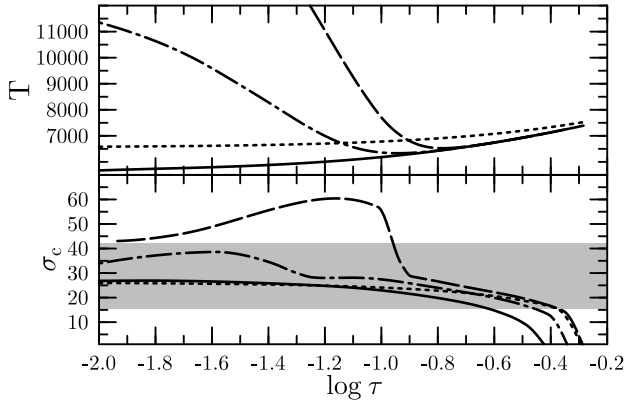


**Figure 4.** Dependence of the characteristic frequency  $\sigma_c$  (bottom panel) in the superficial layers on the choice of the  $T-\tau$  relation (top panel) in the atmosphere of the star. The case of dipole modes in model B are depicted.

processes which act in the stellar atmospheres to sufficiently increase the acoustic cut-off frequency. Shibahashi & Saio (1985) computed critical frequencies for Eddington-type atmospheres as well as for  $T-\tau$  relations fitted to more detailed Kurucz atmospheres. Their fitted solutions showed a larger ratio of  $T_{\text{eff}}/T(\tau=0)$  than in the Eddington atmospheres. For none of the chosen  $T-\tau$  functions, however, a  $\sigma_{\text{ac}}$  resulted that would lead to fully reflected roAp-relevant oscillation modes. The results of an observational determination of the  $T-\tau$  relation of a roAp star were presented by Matthews et al. (1996). Their studied star, HR 3831, indicated an even steeper temperature drop close to the photosphere and a more isothermal behaviour at small optical depths than what Shibahashi & Saio (1985) suggested. [It is, however, noteworthy that Kurtz & Medupe (1996) in their analysis of frequency-dependent oscillation amplitudes conclude that a  $T-\tau$  relationship cannot be derived from roAp oscillation data.] A list of theoretical suggestions to increase  $\sigma_{\text{ac}}$  at the outer boundary of the stellar models was given in section 5 of Shibahashi (1991).

To simulate the effect of roAp-type chemical inhomogeneities on the characteristic frequencies, in particular on the atmospheric cut-off frequency, we studied sharp  $\mu$  transitions in atmospheres with standard  $T-\tau$  relations. According to equation (3), the floating on the top of the stellar atmosphere of rare earth elements leads to a  $\mu$ -inversion. The magnitude and the location of such  $\mu$ -jumps were guided by results of Michaud (1980). Our atmospheric  $\mu$  variations led to  $\sigma_c$  depressions which had no noticeable influence on the amount of energy leakage of the waves with frequencies above the cut-off frequency. Acoustically, the feature was found to be too shallow to be noticed even by high-frequency  $p$  modes.

We postulate now a mechanism that rather successfully increased  $\sigma_c$  in our models. It remains to be seen, however, if it is indeed realized in nature: Since roAp stars have a convection zone which reaches the photosphere and since they have strong magnetic fields, we suggest that roAp stars are capable of building up – very much like solar-type stars – a chromosphere of some extent. This chromosphere goes along with a temperature inversion which we ad hoc parametrized by:

$$T(\tau) = 0.931T_{\text{eff}}[\tau + 0.72858 - 0.3367 \exp(-2.54\tau) + 10 \exp(-50\tau) - 1.0 \exp(-500\tau)]^{1/4}. \quad (2)$$

The above choice is motivated by the Shibahashi & Saio (1985) fit (full line in Fig. 4) except that the first coefficient in the square bracket is adapted to enforce  $T(\tau = 2/3) = T_{\text{eff}}$ . The positive sign in

front of the  $\exp(-50\tau)$  coefficient of equation (2) induces a temperature inversion at small optical depths (dash-dotted line in Fig. 4). Replacing this term by  $+120 \exp(-40\tau)$  leads to the stronger temperature inversion delineated with the dashed line. Finally, the dotted line in Fig. 4 indicates the run of an Eddington-type  $T-\tau$  relation.

We can understand the effect of the temperature inversion on the  $p$ -mode cavity by approximating  $\sigma_c$  for acoustic modes close to the surface:

$$\begin{aligned} \sigma_c &\approx \frac{V}{3} \left( \frac{d \log \rho}{d \log P} - \frac{1}{\Gamma_1} \right) \\ &= \frac{V}{3} \left( \alpha - \delta \nabla_T + \frac{\varphi}{\delta} \nabla_\mu - \frac{1}{\Gamma_1} \right). \end{aligned} \quad (3)$$

We used  $\alpha = (\partial \log \rho / \partial \log P)_T$ ,  $\delta = -(\partial \log \rho / \partial \log T)_P$ , and  $\nabla_T \equiv d \log T / d \log P$  to be the effective temperature gradient. A negative  $\nabla_T$  clearly increases the critical frequency for adiabatic  $p$  modes. Quantitative effects are displayed in Fig. 4.

The temperature inversions shown in Fig. 4 are, admittedly, rather strong. In particular, we have to face the fact that no observational signature for chromospheric activity has been found to date (e.g. Shore et al. 1987). Therefore, the conjectured temperature inversion cannot be very strong because it should have been observable through emission-line features otherwise. Notice, however, that only the innermost part of the above temperature inversions are essential for the increase of  $\sigma_c$ . Hence, a levelling off of the temperature after an increase of 3000 K at most is sufficient to completely reflect the roAp-type acoustic waves in many cases.

In the next section we investigate the effect of this modified outer edge of the cavity on the stability properties of high-order  $p$  modes. As of now, the physics of their excitation remains a matter of debate.

### 3.2 Excitation physics

Since the roAp star domain on the HR diagram appears to overlap with the  $\delta$  Sct stars (see Fig. 1), the partial He<sup>+</sup> ionization zone was thought for a long time to be also the driving agent for roAp stars (e.g. Kurtz 1990; Matthews 1997). Numerical computations never supported this conjecture, however. Based on the compositional peculiarity of the roAp stars, Matthews (1988) hypothesized, relying on qualitative microphysical arguments, that Si iv partial ionization might provide sufficient  $p$ -mode driving even if He was drained out of the potential driving depth in the star. He estimated an overabundance of Si iv in the superficial stellar regions of the order of 200 to be sufficient for the mechanism to work. A completely different avenue was taken by Shibahashi (1983) which was also investigated by Cox (1984). Their local analyses of oscillatory magneto-gravity waves suggested overstability under favourable circumstances. They expected the magnetic polar regions to become overstable under Ap-star circumstances. The eventually observable roAp star oscillation are those global  $p$  modes which are resonantly excited by the overstable magneto-gravity waves. This picture has the great advantage of naturally explaining the alignment of the pulsation axis with the magnetic axis and the selection of axisymmetric modes. Detailed global analyses which are necessary to settle the excitation problem eventually are, however, lacking also for this approach. Recently, Dziembowski & Goode (1996) noted that the partial H ionization contributes positively to the work integral. No  $p$  mode with a roAp-star relevant period was found yet destabilized by the  $\kappa$  mechanism.

If a ‘thermomechanical valve mechanism’ is to power roAp-like oscillation modes, then the oscillation periods have to be of the

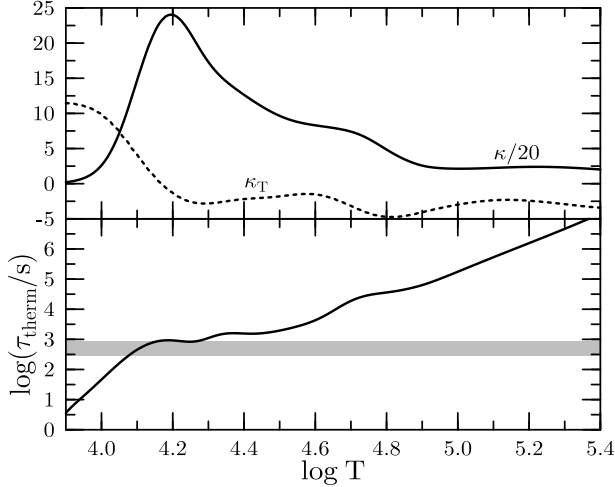


**Figure 5.** Spatial run of  $\kappa_T$ , a scaled  $\kappa$ , and (in the lower panel) the variation of the thermal time-scale ( $\tau_{\text{therm}}$ ) in model J. The grey shading indicates the temporal region of interest for roAp oscillations (cf. text).

order of the thermal time-scale ( $\tau_{\text{therm}}$ ) of the envelope overlying the driving region (e.g. Cox 1980). The corresponding spatial structure shown in Fig. 5 for stellar model E is representative for the whole model series looked at in this paper. A qualitative inspection of the models shows that those superficial regions with a thermal time-scale below about 1000 s contain the steep  $\kappa_T$  rise towards the surface induced by partial H and He ionization (see Fig. 5). The deeper-lying, potentially driving region for which  $d\kappa_T/dr > 0$  (at  $4.1 \leq \log T \leq 4.8$  in Fig. 5) favours time-scales – as expected – of modes in the  $\delta$  Sct period domain, i.e. above  $10^4$  s. Therefore, we expect – already a priori – partial ionization of H and He to be the prospective excitation agents for roAp-type oscillations.

We computed nonadiabatic oscillation spectra for the stellar models listed in Table 1. The chromosphere-like temperature structure in the atmosphere which we introduced provided a sufficiently high acoustic cut-off so that the acoustic cavity appears reflective at the surface for most of the computed oscillation modes. The numbers of overstable  $p$  modes in the different models are listed in Table 2. For the  $\delta$  Sct-type oscillation modes we indicate only if we found any (‘x’ in Table 2) or none (‘-’ in Table 2). Selected, results are discussed in the following to demonstrate their properties and the physical mechanisms.

Fig. 6 shows the whole dipole  $p$ -mode domain in which overstable oscillation modes were found for the  $1.6-M_{\odot}$  models. The imaginary parts of the eigenfrequencies were suitably scaled to accommodate the large numerical range of  $\sigma_1$  in the short- and long-period domain. We defined:

$$\Sigma_1 \equiv \text{sign}(\sigma_1) \log \left( 1 + \frac{|\sigma_1|}{1 \times 10^{-4}} \right). \quad (4)$$

Negative  $\Sigma_1$  values represent overstable modes. Values of  $\Sigma_1$  exceeding unity behave essentially logarithmic whereas smaller values are linear in  $\sigma_1$ .

The full line in Fig. 6 (as well as in other figures showing the three

evolutionary stages of a selected stellar mass) stands for the zero-age main-sequence (ZAMS) model, the dotted line represents the slightly evolved model close to the first turn-around, and the dashed-dotted line depicts the results of the most evolved stage. For all models in Fig. 6 we used the weak temperature inversion. The  $1.6-M_{\odot}$  ZAMS model is pulsationally stable over the whole frequency domain (i.e. roAp and  $\delta$  Sct modes). The more evolved models show a short-period instability around 500 s (the number of overstable modes is listed in Table 2) as well as overstable long-period modes above 3600 s, which are appropriate for  $\delta$  Sct variables. For both stellar models (H and I) the range of overstable roAp-type modes remains unchanged. This is different in the case of a strong T-inversion in the  $1.5-M_{\odot}$  sequence, which is shown in Fig. 7. In this case the instability domain shifts to longer periods as the star evolves. On the ZAMS, periods around 400 s are excited where the subgiant model has four overstable  $p$  modes around 750 s.

In all models with overstable high-order  $p$  modes we found only a few of them (cf. Table 2) at a selected spherical degree. This short-period instability domain is always separated from the long-period domain with low-order  $p$  modes which are typical for  $\delta$  Sct variability. It is only in the  $1.5-M_{\odot}$  ZAMS model where even this longer-period instability range extends to below 1000 s.

To study the destabilisation of the  $p$  modes we plotted some relevant physical quantities of model H as a function of depth in the envelope (parametrized by the total pressure) in Fig. 8. The top panel shows the opacity derivatives along the chosen thermodynamic basis. It was argued in Unno et al. (1989) that a necessary condition for pulsational driving requires

$$\frac{d}{dr} \left( \kappa_T + \frac{\kappa_p}{\Gamma_3 - 1} \right) > 0. \quad (5)$$

The major contributor to the above sum is clearly  $\kappa_T$ . The outer potential driving region is due to partial H and He ionization. The second, deeper lying one is associated with the  $\text{He}^+$  partial ionization. We see that the long-period mode is mainly driven by  $\text{He}^+$  ionization, the outer ionization zone is actually damping in this case. The high-order ( $k = 34$ ) dipole mode, on the other hand gets all the driving from the H/He ionization zone. The deeper lying regions are all slightly damping. The results displayed in Fig. 8 agree very well with the rather qualitative reasoning on the potential driving agent for roAp modes used before. Notice, however, that the condition in equation (5) was derived for weakly non-adiabatic circumstances. Therefore, noticeable deviations from this simple form must be expected occasionally.

### 3.3 Inhomogeneous envelopes

A persistent problem with the classical  $\kappa$  instability mechanism found above is that not only short-period modes of high radial order are excited, but also the  $\delta$  Sct-type low-orders. Observations clearly show that  $\delta$  Sct-like oscillations are not present in roAp stars.

To suppress the  $\delta$  Sct-type modes we assumed a drainage of He from the superficial regions. Stabilization of turbulent bulk motion by the magnetic field might cause such a He depletion in the outer parts of Ap-star envelopes (Vauclair & Vauclair 1982). We assumed

**Table 2.** Excited dipole modes of roAp and  $\delta$  Sct type for weak (first entry) and strong (second entry) T-inversions and homogeneous envelope compositions.

Period domain	A	B	C	D	E	F	G	H	I	J	K	L
roAp	0,0	0,0	0,0	0,0	0,0	0,0	0,0	3,3	3,2	1,3	5,4	4,3
$\delta$ Sct	-, -	x, x	x, -	x, x	x, x	-, -	x, -	x, -	x, -	x, x	x, x	x, x

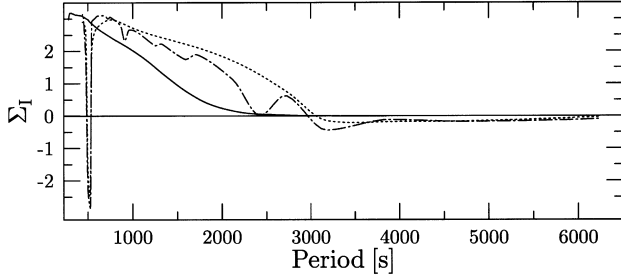


**Figure 6.** Appropriately scaled imaginary parts of  $p$  modes for the 3 models of the  $1.6M_\odot$  sequence with the weak temperature inversion. Full line: model G, dotted line: model H, and dashed-dotted line: model I.

ad hoc that the He drainage extends over those layers where magnetic pressure (for a kilogauss field) exceeds gas pressure. We depleted helium to a mass fraction of 0.1 (and enhanced H to 0.88) at temperatures below  $\log T = 4.5$  (cf. Fig. 2). Across a transition region of  $\Delta \log T = 0.1$  our canonical population I composition of  $X = 0.7, Y = 0.28$  was recovered. For ease of computation, the smooth transition was prescribed by a hyperbolic tangent function. Fig. 2 indicated already that only an extremely thin mass layer is affected by the drainage. In models H, K, and L for which we performed this experiment the He drainage extended over the outer  $4 \times 10^{-9} M_\odot$ . Notice that this is six orders of magnitude less than what Shibahashi & Saio (1985) adopted in their study.

The repeated non-adiabatic stability calculations on models H, K, and L showed that the long-period instabilities disappear if the superficial layers are chemically inhomogeneous. The effect is less pronounced in model H than in the two  $1.5-M_\odot$  ones, however. Additionally, the oscillation modes of the strong temperature-inversion models seem to react more strongly to inhomogeneity than those with the weak inversions. The dipole-mode results of model K are shown in Fig. 9. The long-period modes above about 1200 s which are overstable in the model with chemically homogeneous envelope (broken line) are all stabilized in the He-drained one (full line). The short-period modes remain overstable. The radial orders of the overstable modes are, however, lower in the inhomogeneous envelope: in the homogeneous outer layers, periods around 500 s are excited whereas periods of about 750 s are favored in the inhomogeneous case. This property is not generic, however. In other cases, such as model L, the short-period instability domain remained unchanged. A peculiarity of this model L was that in addition to the short-period instability a dipole-mode at about 900 s turned overstable in the inhomogeneous envelope model. In other words, we had one case where *non-successive* radial orders were excited. We show the corresponding diagram in Fig. 10.

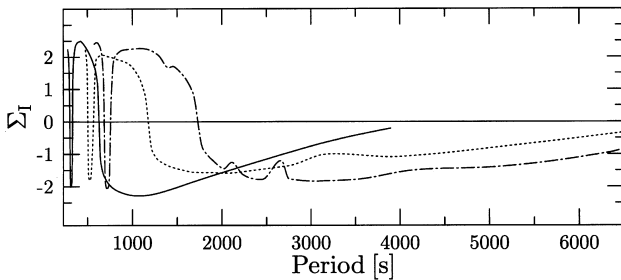


**Figure 7.** Appropriately scaled imaginary parts of  $p$  modes for the three models of the  $1.5-M_\odot$  sequence and a strong temperature inversion. Full line: model J, dotted line: model K, and dashed-dotted line: model L.

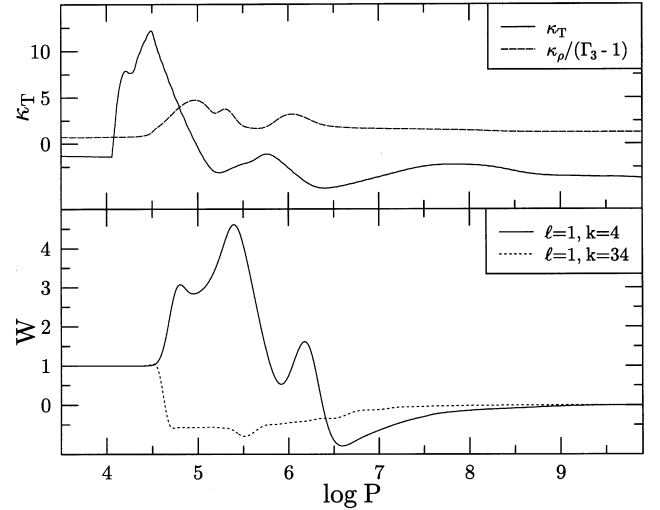


**Figure 8.** Top panel shows the spatial run of the opacity derivatives which enter the computation of the work integral. The lower panel displays the cumulative work done by a short-period (dashed line) and a long-period (full line) mode, both of which are overstable.

To see where the loss of the  $\delta$  Sct modes in inhomogeneous envelope models comes from, we look at the work integral for the  $k = 9$  dipole mode with a period of 3560 s of model L. In the homogeneous envelope model this mode is overstable but it is damped in the inhomogeneous one. Fig. 11 displays in the lower panel the cumulative work; the solution for the homogeneous case is delineated with the full and the inhomogeneous one with the dashed line. Both work integral curves are independently normalized to unity at the surface. Obviously, the hydrogen partial ionization zone contributes to driving in the homogeneous but damps in the inhomogeneous envelope, and it is the action of this region which decides over stability or overstability. We attribute the swapping of the work contribution of the H-ionization zone to the influence of the different envelope structures. Notice that the  $\kappa_T$  runs are very close in both cases. Therefore, it is the phase relation between density and pressure perturbation at the H-ionization zone which cause the difference. Notice once more that that He drainage extends only to  $\log P \approx 5$ .

### 3.4 Dependence on spherical degree

Observed frequency spectra of roAp stars hint at the possibility that not only dipole modes are involved in their light variability. In some cases – such as HR 1217, HD 119027, HD 203932 – the frequency

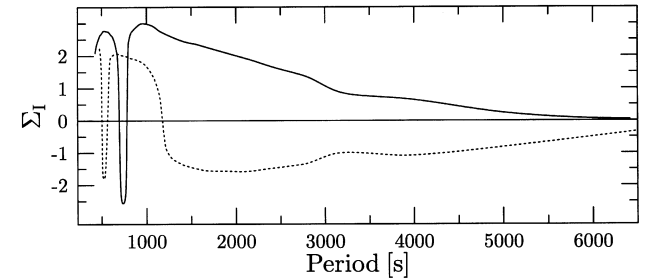


**Figure 9.** The run of  $\Sigma_I$  as a function of period for model K with strong temperature inversion. The full line shows the results for the inhomogeneous envelope. The dashed line depicts the behaviour of oscillation modes in the model with homogeneous outer layers.

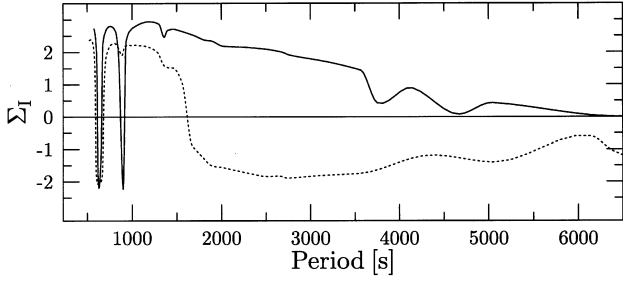


**Figure 10.** The run of  $\Sigma_1$  as a function of period for model L with weak temperature inversion. The full line shows the results for the inhomogeneous envelope. The dashed line depicts the behavior of oscillation modes in the model with homogeneous outer layers. In the inhomogeneous case, non-successive overstable radial orders exist.

spacings are not even enough to be explainable with  $\ell = 1$  modes only (Kurtz 1995). Also from the theoretical side, assuming now that a classical  $\kappa$  mechanism drives the modes, we expect not only  $\ell = 1$  modes to be excited.

Fig. 12 shows results for the inhomogeneous model L with weak temperature inversion. We plotted directly the imaginary parts of the eigenfrequencies for radial orders 33 to 37. The highest order which becomes overstable at  $\ell = 1$  is 36. Lower orders tend to have their maximum driving at higher degrees. From the asymptotic relation  $\nu_{k\ell} \propto \nu_0(k + \ell/2 + \varepsilon)$  we deduce that the maximum driving occurs always at similar period, irrespective of the spherical degree. Our computations showed that a mix of different spherical degrees should contribute to the roAp variability. As it is monitored mainly photometrically at the moment, spherical degrees higher than 3 are not very relevant. Adding up all the low- $\ell$  (0 to 3) modes and the different radial orders, we found that usually less than 12 modes (in terms of the principal quantum numbers  $k$  and  $\ell$ ) are simultaneously excited.

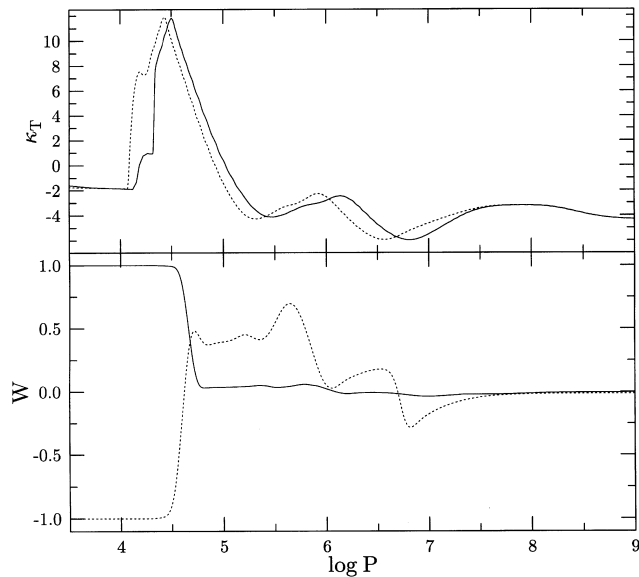


**Figure 11.** Effect of He drainage in the outermost part of the envelope on the work integral of  $\ell = 1, k = 9$  mode. The full line depicts the solution on the homogeneous envelope. The dashed line stands for the one on the chemically inhomogeneous envelope.

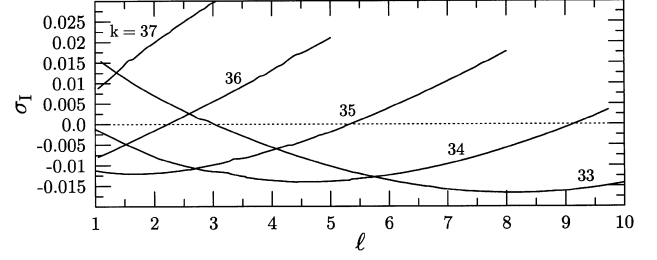


**Figure 12.** Imaginary parts of high-order  $p$  modes of model L as a function of spherical degree.

### 3.5 Node distribution in the atmospheres

For recent spectroscopic observations of  $\alpha$  Cir, phase shifts in the temporal behaviour of absorption-line features which probe different depths in the atmosphere suggested that a node is lying in the optically thin superficial layers (Baldry et al. 1998). We analysed our eigensolutions in this respect. Fig. 13 shows the overstable dipole modes of model H. The upper panel depicts displacement eigenfunctions. They do not shift significantly for successive radial orders. In all three cases displayed, a node lies at very low optical depths and a second one close to  $\tau = 2/3$ . The situation is different for the temperature perturbation for which the real part of the eigenfunction is shown in the lower panel of Fig. 13. The  $k = 35$  mode shows a node at small optical depths, whereas the next two lower-order modes have no node at  $\tau < 2/3$ . The reason for the temperature perturbation to have a stronger variation than the displacement function is the very superficial H/He ionization zone. This region causes, as a result of a strong entropy perturbation, an associated strong temperature variation.

We emphasize that our treatment of the outer regions, in particular of the optically thin regions are far from realistic. Therefore, the results in Fig. 13 should at best be taken as indications that indeed nodes can be expected in the atmospheres of roAp stars. Quantitative aspects will certainly change when studies concerning this issue are performed with the correct perturbed transport equations. Only then can we expect to exploit this property of roAp stars for atmospheric diagnosis.

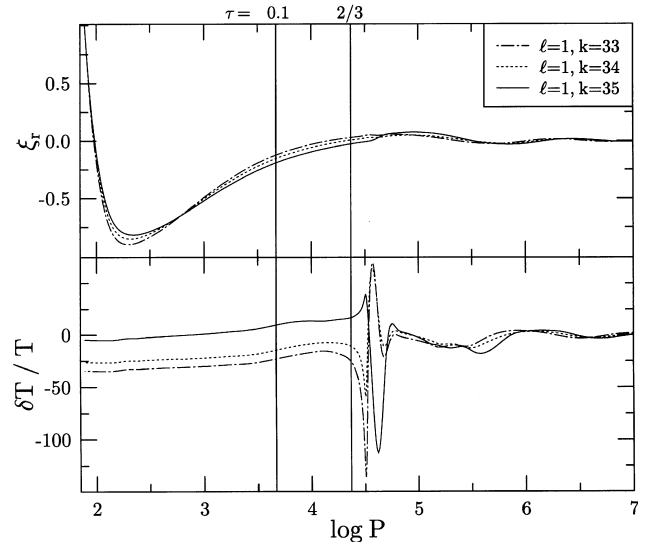


**Figure 13.** Spatial behaviour of eigenfunction in the outermost layers for the three overstable high-order dipole modes of model H.

#### 4 DISCUSSION

Non-adiabatic stability analyses applied to evolutionary models with homogeneous Population I composition revealed that the  $\kappa$  mechanism of H/He ionization can destabilize short-period roAp-type modes. We found the short-period instabilities to be restricted to the 1.5- and 1.6- $M_{\odot}$  sequences. The rough location of the blue edge for the high-order roAp oscillations lies, according to our preliminary computations, at about  $\log T_{\text{eff}} = 3.86$ . Both, main-sequence and early subgiant models can become roAp pulsators. In contrast to a recent mapping of roAp stars onto the HR plane (North et al. 1997), we find our overstable models to have somewhat lower masses and to have lower effective temperatures than what the North et al. (1997) data imply. On the other hand, we expect the blue edge to shift to higher temperatures if the more helium (than what we assumed in our computations) is depleted from the most superficial stellar layers. In this case the H driving in the H/He I partial ionization zone should get more efficient. This has to be proven, however, with explicit computations in the future.

In contrast to  $\delta$  Sct stars, H/He ionization dominates the driving of the roAp modes. Since the H/He ionization zone lies at lower temperatures than the He<sup>+</sup> one, we expect the blue edge of the roAp instability domain to be *somewhat* cooler than that of  $\delta$  Sct stars (cf. Fig. 1).

In all cases, the number of overstable oscillation modes we counted in our computations was small. Not more than five overstable modes of a given spherical degree were encountered. This is still larger than what is observed in some roAp stars so that mode selection remains a problem to be addressed. In contrast to  $\delta$  Sct stars, however, the number of overstable modes is considerably smaller in roAp models. From Fig. 5 we see that at the base of the  $\kappa_T$  gradient induced by H/He partial ionization the thermal scale levels off at about 1000 s. Only periods with shorter periods can be potentially excited in this region. As the overtones are already high, the radiative dissipation is also high. Therefore, it seems that only for a few modes with high radial order can H/He driving overcome the radiative dissipation anymore.

A necessary prerequisite for short-period oscillations to be excited was the hypothesis of a temperature inversion in the inner atmosphere of the models. The temperature inversion which raises the superficial critical frequency sufficiently to reflect roAp-type modes need not be very high. Depending on the steepness, one to three thousand K are enough. Another effect of the steepness of the inversion is that it influences the number of excited modes.

The evolutionary stage of roAp stars can be anywhere between the main sequence and the beginning of the subgiant stage – observed frequencies do allow for this bandwidth of dating. In the most advanced phases of evolution the core is no longer convective. Therefore, no magnetic dynamo could be operative anymore; most of the star – except for the narrow ionization regions – is radiative. If the cyclic secular frequency variations of roAp stars were interpreted to be owing to some magnetic activity cycle then the ohmic decay time of the stellar magnetic field would limit the maximum age of such roAp stars. At present, the origin of the frequency variations as observed by now in HD 134214 and HR 3831 (Kurtz et al. 1994; Kreidl et al. 1994; Kurtz et al. 1997) is far from clear.

From our computations we cannot unambiguously attribute an evolutionary stage to the range of periods of overstable oscillation modes. From Fig. 7 we see a tendency of longer periods to be excited at later evolutionary stages in the 1.5- $M_{\odot}$  models. This finding could, however, not be reproduced in the 1.6- $M_{\odot}$  models.

Introducing an atmospheric temperature inversion in the models eventually produced the long elusive overstable roAp-type modes. However, in the same models we found roAp and  $\delta$  Sct modes excited – this contradicted observational evidence. Therefore, we argued for a He drainage in these superficial regions where magnetic pressure dominates over gas pressure. When assuming a kilogauss dipole field we found a mass fraction of only a few times  $10^{-9}M_{*}$  to be magnetically dominated and hence drained from He. In such models we got rid of the  $\delta$  Sct modes but could retain the roAp ones. As only the the H/He ionization was deficient of He, it is evident that H ionization dominates the excitation of roAp modes (see also the work integrals in Fig. 8). Notice that the He<sup>+</sup> partial ionization is *not* modified in these models, but still we got rid of the  $\delta$  Sct-type modes. This contradicts previous reasoning (Cox, King & Hodson 1979). Our computations of inhomogeneous models showed that for  $\delta$  Sct-type modes the H/He ionization zone has a damping influence which even over-compensates the driving action of the He<sup>+</sup> region. Furthermore, observations support our picture which emphasizes the rôle of the magnetic field for the presence of high-frequency (roAp-like) oscillation modes which are not found in  $\delta$  Sct stars such as in FG Vir (Breger et al. 1996).

In some of the inhomogeneous models we found excited non-successive overtones. Such a behaviour is reminiscent of the frequency spectrum as found for example in HD 217522 (Kurtz 1995).

A major problem with whole stability analysis as presented here remains: the driving region of the roAp modes reaches into the region where the magnetic pressure dominates the star, therefore we must expect a non-vanishing influence of the perturbed magnetic field. In other words, magneto-acoustic modes might be excited which carry away energy (Roberts & Soward 1983; Dziembowski & Goode 1996). If such an interaction is efficient enough it can damp out the pure acoustic modes of which we were talking here. However, at the moment we are not in a position to do such a non-adiabatic analysis quantitatively. Dziembowski & Goode (1996) presented estimates of such an interaction in the adiabatic limit. From their results we expect that only the very strongest excited modes might survive in the correct hydro-magnetic treatment.

Martinez (1996) discussed an unusual, possible roAp star – HD 75425 – which oscillates with 30-min period. This period is significantly longer than what is found for roAp stars and somewhat short for  $\delta$  Sct stars. Referring to Fig. 7 we find that such long periods could indeed be excited. For them the action of the He<sup>+</sup> is important, however. If we interpret HD 75425 in our framework, it should either be rather young so that sedimentation was not yet efficient enough or the stabilization of the flow by the magnetic field is not sufficiently strong. The latter alternative would require a magnetic field which is weaker than what is usually found in other roAp stars. It is, however, not yet clear *why* no high-order modes are present in HD 75425. Either they have not yet been seen and they are actually hidden (at even lower amplitude) in the long-period data or the hypothesized temperature inversion is not strong enough to trap the high-order  $p$  modes.

It appears highly rewarding to search for weakly magnetic A-type stars to see if it is possible at all to have both period domains (cf. Figs 6 and 7) excited in any such stars. To extend our speculations further in this direction we mention Am–Fm stars (Kurtz et al. 1995; Kurtz 1998). These mildly peculiar cool main-sequence stars seem to be always binaries. Sedimentation of elements owing to suppressed rotational velocities might eventually suppress  $\delta$  Sct pulsations. Since the chemical peculiarity is not associated with a magnetic field these stars cannot build up a



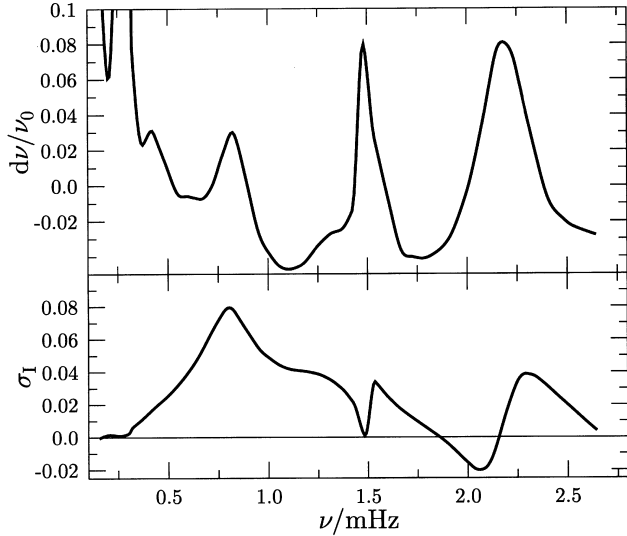


**Figure 14.** Relative deviation of the frequency spacing from the asymptotic value for model K.

sufficiently high critical frequency to support roAp-type modes. Therefore, we do not expect Am–Fm stars to be seen as short-period pulsators; on the other hand, if He drainage is not strong yet (i.e. if they are young enough) they might well be  $\delta$  Sct type pulsators (cf. Cox et al. 1979).

As mentioned before, we were able to enhance the critical frequency at the stellar surface by ad hoc postulating a temperature inversion in the optically thin regions of the stellar atmosphere. Physically, this is equivalent to assuming a chromosphere in these stars. The spectral types of the roAp stars are just at the border where chromospheric evidence starts to be observed. According to prevailing theoretical ideas, the roAp stars provide already the necessary ingredients for chromospheric heating: a superficial convection zone and strong magnetic fields which might provide the necessary acoustic flux and possible magneto-acoustic waves, respectively. Shore et al. (1987) found, however, no signs of chromospheric emission in roAp stars. For further progress it would be highly rewarding to find observational evidence for or against the temperature-inversion hypothesis.

The appendix discussed the approach of non-adiabatic frequencies to what is expected from adiabatic asymptotics. We found that caution is required when using high-frequency oscillation data to infer stellar parameters. Even if the excitation rates of high-order modes are low, the deviations of frequency spacings from the adiabatically predicted ones can be up to about 8 per cent (see Fig. 14). Furthermore, this behavior is expressedly non-monotonic so that an easy correction cannot be applied. The magnitude of nonadiabatic frequency shifts in roAp stars is not negligible compared with the magnetic-field induced frequency perturbations (Dziembowski & Goode 1996). Therefore, asteroseismology of roAp stars is quite a challenge for pulsation theory. To finish, we feel that a warning of simple application of adiabatic asymptotics to high-order modes is also in place for solar seismology.

## ACKNOWLEDGMENTS

Financial support by the Swiss National Science Foundation through a PROFIL2 fellowship (AG) is gratefully acknowledged. For part of this work, HS was supported by the Swiss National Science Foundation and the Japan Society for the Promotion of

Science. Enlightening discussions with and constructive refereeing of the manuscript by D. Kurtz as well as the initial motivation by H. Shibahashi were of great help. W. Löffler kindly provided most of the stellar models used for the analyses.

## REFERENCES

- Alecian G., 1986, in Cowley C. R., Dworetzky M. M., Megessier C., eds, Upper Main Sequence Stars with Anomalous Abundances. Reidel, Dordrecht, p. 381
- Baldry L. K., Viskum M., Bedding T. R., Kjeldsen H., Frandsen S., 1998, preprint
- Breger M. et al., 1996, A&A, 309, 197
- Brown T. M., Christensen-Dalsgaard J., Weibel-Mihalas B., Gilliland R. L., 1994, ApJ, 427, 1013
- Christensen-Dalsgaard J., 1988, in Christensen-Dalsgaard J., Frandsen S., eds, Proc. IAU Symp. 123, Advances in Helio- and Asteroseismology. Reidel, Dordrecht, p.295
- Cox A. N., King D. S., Hodson S. W. 1979, ApJ, 231, 798
- Cox J. P., 1980, Theory of Stellar Pulsation, Princeton Univ. Press, Princeton
- Cox J. P., 1984, ApJ, 280, 220
- Dziembowski W. A., Goode P. R., 1996, ApJ, 458, 338
- Gabriel M., Noels A., Scuflaire R., Mathys G., 1985, A&A, 143, 206
- Gautschi A., Ludwig H.-G., Freytag B., 1996, A&A, 311, 493
- Heller C. H., Kawaler S. D., 1988, ApJ, 329, L43
- Kreidl T. J., Kurtz D. W., Schneider H., van Wyk F., Roberts G., Marang F., Birch P. V., 1994, MNRAS, 270, 115
- Kurtz D. W., 1978, Inform. Bull. Var. Stars, 1436
- Kurtz D. W., 1990, ARA&A, 28, 607
- Kurtz D. W., 1995, in Ulrich R.K., Rhodes E. J., Jr, Däppen W., eds, ASP Conf. Ser. Vol.76, GONG '94: Helio- and Asteroseismology. Astron. Soc. Pac., San Francisco, p. 606
- Kurtz D.W., 1998, in Pradley P. A., Guzik J. A., eds, Asp Conf. Ser. Vol. 135, A Half Century of Stellar Pulsation Interpretations, Astron. Soc. Pac. San Francisco, p. 420
- Kurtz D. W., Medupe R., 1996, Bull. Astr. Soc. India, 24, 291
- Kurtz D. W., Wegner G., 1979, ApJ, 232, 510
- Kurtz D. W., Schneider H., Weiss W. W., 1985, MNRAS, 215, 77
- Kurtz D. W., Martinez P., van Wyk F., Marang F., Roberts G., 1994, MNRAS, 268, 641
- Kurtz D. W., Garrison R. F., Koen C., Hofmann G. F., Viranna N. B., 1995, MNRAS, 276, 199
- Kurtz D. W., van Wyk F., Roberts G., Marang F., Handler G., Medupe R., Kilkeny D., 1997, MNRAS, 287, 69
- Martinez P., 1996, Inf. Bull. Var. Stars, 4348
- Mathys G., Hubig S., 1997, A&AS, 124, 475
- Matthews J. M., 1988, MNRAS, 235, 7P
- Matthews J. M., 1997, in Provost J., Schmider F.-X., eds, Proc. IAU Symp. 181, Sounding Solar and Stellar Interiors. Kluwer, Dordrecht, p.387
- Matthews J. M., Wehlau W. H., Rice J., Walker G. A. H., 1996, ApJ, 459, 278
- Michaud G., 1980, AJ, 85, 589
- North P., Jäschek C., Hauck B., Figueras F., Torra J., Künzli M., 1997, in *Hipparcos* Venice '97, ESA SP-402, 239
- Roberts P. H., Soward H.M., 1983, MNRAS, 205, 1171
- Shibahashi H., 1983, ApJ, 275, L5
- Shibahashi H., 1991, in Gough D., Toomre J., eds, Challenges to theories of the structure of moderate mass stars. Springer, Berlin, p.303
- Shibahashi H., Saio H., 1985, PASJ, 37, 245
- Shore S. N., Brown D. N., Sonneborn G., Gibson D. M., 1987, A&A, 182, 285
- Stibbs D. W. N., 1950, MNRAS, 110, 395
- Unno W., Osaki Y., Ando H., Saio H., Shibahashi H., 1989, Nonradial Oscillations of Stars. Univ. of Tokyo Press, Tokyo
- Vauclair S., Vauclair G., 1982, ARA&A, 20, 37

## APPENDIX A

We discuss concisely the effects of non-adiabaticity on the oscillation-frequency spectrum and compare it with adiabatic results. This

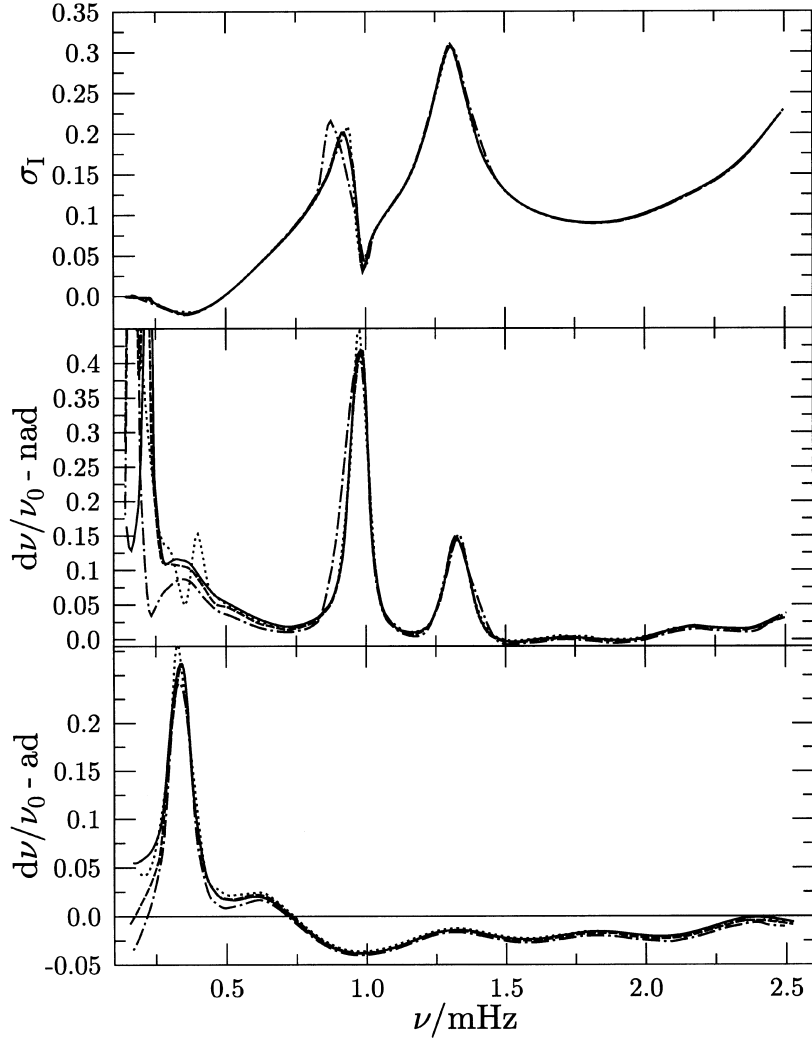


**Figure A1.** Frequency behaviour for model B. The top diagram shows the imaginary parts of the non-adiabatic eigenvalues. The values for degrees  $1 \leq \ell \leq 4$  are plotted on top of each other. The middle panel shows the fractional deviation of the non-adiabatic frequency spacing from the asymptotic value. The lowest panel shows the same deviation computed from the adiabatic frequencies. The line coding is as following:  $\ell = 1$ : full line;  $\ell = 2$ : dotted line;  $\ell = 3$ : dashed line;  $\ell = 4$ : dash-dotted line.

is mainly of interest for those aiming at using roAp frequency data for seismological deductions.

For high radial-order modes of low degree, the frequency separation of equal-degree modes is usually rather close to

$$\frac{1}{\nu_0} = 2 \int_0^{R_*} \frac{dr}{c_{\text{ad}}} \quad (\text{A1})$$

with the adiabatic sound speed given by  $c_{\text{ad}} \equiv \sqrt{\Gamma_1 P / \rho}$  (cf. Section 3.4). The value of  $\nu_0$  corresponds to the frequency of an acoustic wave to travel across a star.

In the following we investigate how quickly the frequency separation approaches the asymptotic limit which is frequently referred to for asteroseismic purposes. To quantify the relative deviation of the actually computed frequency spacing from the expected one ( $\nu_0$ ), we introduce

$$\frac{d\nu}{\nu_0} = 1 - \frac{\nu_{k+1} - \nu_k}{\nu_0}. \quad (\text{A2})$$

Fig. A1 shows extensive results for model B for which we computed oscillation modes with spherical degree 1 (full line), 2

(dotted line), 3 (dashed line), and 4 (dash-dotted line) for many radial orders. Computations were performed adiabatically as well as non-adiabatically. The bottom panel of Fig. A1 displays the relative deviation  $d\nu/\nu_0$  of the adiabatic frequency spacing as a function of the oscillation frequency. Above about 1.3 mHz the deviation from the asymptotic value (51.46  $\mu\text{Hz}$ ) drops below 2 per cent for all degrees. In the range between 2.25 and 2.5 mHz, where many roAp modes are observed, the adiabatic mode separation agrees with the asymptotic value on the level of 0.1 to 1 per cent, depending on the degree. This frequency range corresponds to radial orders exceeding 40.

To see if the convergence properties of the non-adiabatic eigenfrequencies are comparable with the adiabatic ones we plot the relative deviation from the asymptotic value (adiabatically computed) in the middle panel of Fig. A1. The most obvious discrepancy is seen around 1 and 1.3 mHz. There we find a relative deviation of the spacing of 40 and 10 per cent, respectively. These two features are clearly associated with the local maxima in the damping rates  $\sigma_I$  which are shown in the top panel of Fig. A1. In the frequency range between 1.5 and 2 mHz, the frequency separation

relaxes to within a few per cent of the asymptotic one. For higher frequencies, however, they start to diverge again in accordance with the rise of the damping rates.

What relevance does this behaviour have for roAp modes? After all, the modes which we used for the above demonstration were all damped. We consider now the relative deviation  $d\nu/\nu_0$  of the non-adiabatic oscillation frequency separation from the the adiabatic asymptotic value for  $\ell = 1$  of model K. This model has four overstable modes around 500 s period. The imaginary parts are rather small but still the frequency spacing reacts sensitively to the  $\sigma_1$  variation. Fig. 14 shows that at 1.5 mHz – at the position of a marginally overstable oscillation mode for which the damping rate is close to zero – the frequency spacing deviates by about 8 per cent

from the adiabatically expected one. In the overstable period domain, the frequency spacings change from 3 per cent longer to 8 per cent shorter than the predicted asymptotic frequency spacing. For seismological inferences such differences can be relevant.

To finish, we emphasize that, if high accuracy is crucial, non-adiabaticity effects are not negligible in deriving stellar parameters from high-frequency oscillation data. This conclusion might not only apply to roAp stars but also to the high-frequency domain of solar oscillations.

This paper has been typeset from a  $\text{T}_E\text{X}/\text{L}^A\text{T}_E\text{X}$  file prepared by the author.